

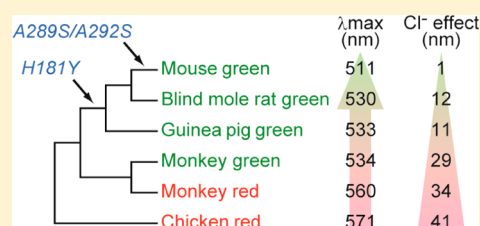
Chloride-Dependent Spectral Tuning Mechanism of L-Group Cone Visual Pigments

Takahiro Yamashita, Shuhei Nakamura, Kei Tsutsui,[†] Takefumi Morizumi,[‡] and Yoshinori Shichida*

Department of Biophysics, Graduate School of Science, Kyoto University, Kyoto 606-8502, Japan

S Supporting Information

ABSTRACT: Most vertebrates have one type of rhodopsin and multiple types of cone visual pigments with different absorption maxima in their retinas. The spectral sensitivities of multiple cone visual pigments contribute to color discrimination in these animals. Vertebrate cone visual pigments are classified into four groups based on their amino acid sequences. Among these groups, many pigments in the longer wavelength-sensitive group (L-group) have a unique spectral tuning mechanism, that is, the red-shift of absorption maximum induced by the binding of chloride to His181 of the protein moiety (chloride effect). However, a few pigments such as mouse green and guinea pig green pigments in L-group have a tyrosine residue instead of a histidine at position 181. Interestingly, mouse green shows no chloride effect, whereas guinea pig green shows a significant chloride effect. In the present site-directed mutational analysis, we revealed that this difference in the chloride effect in rodent pigments is completely explained by the replacements of two residues at positions 289 and 292. In addition, mutations at positions 181, 289, and 292 abolished 80% of the chloride effect in monkey red and green. Further analysis with chimeras showed that the residual 20% of the chloride effect could be attributed to helical interactions within the pigments. Thus, we concluded that these three amino acid residues are the main determinants of the chloride-dependent spectral shift in L-group pigments.



In the retinas of most vertebrates, there are two types of photoreceptor cells, rods and cones, which are responsible for scotopic and photopic vision, respectively. Rods contain one type of visual pigment, rhodopsin, whereas cones contain two or more types of cone visual pigments with different absorption maxima.^{1,2} Since the presence of multiple types of cone visual pigments is one of the molecular bases for color discrimination, investigating the spectral tuning mechanism of cone visual pigments has been considered an important topic of vision research. Like the rod visual pigment rhodopsin, cone visual pigments consist of a protein moiety opsin and a chromophore 11-*cis*-retinal and are classified into four groups on the basis of sequence similarities.³ The absorption maximum of a visual pigment is generally determined by the physicochemical properties of amino acid residues surrounding the retinal chromophore. However, L-group cone visual pigments can bind to chloride within the protein moiety and shift the absorption maximum to a longer wavelength.

The chloride-dependent spectral red-shift in L-group pigments is referred to as the “chloride effect”, which was first reported in gecko visual pigment as a representative sample by Crescitelli.⁴ A similar chloride effect was later reported in chicken red pigment (iodopsin).^{5,6} Iodopsin exhibits an absorption maximum at 571 nm in the presence of chloride, but depletion of chloride from the sample solution or its replacement with nitrate causes the absorption maximum to shift to about 530 nm.⁷ UV-vis and FTIR spectroscopic studies of iodopsin showed that chloride and nitrate stabilize the different conformations near the chromophore-binding site of iodopsin, although these anions bind to the protein moiety

competitively with each other.^{8,9} It should also be noted that the anion-free form of iodopsin has a chromophore conformation very similar to that of the nitrate-bound form. Site-directed mutagenesis experiments of human red and green pigments by Oprian's group revealed that His181 and Lys184 (in the bovine rhodopsin amino acid numbering system) contribute to the chloride binding and His181 is the primary residue for the chloride effect.¹⁰ These residues are located in the second extracellular loop (ECL2) and are well conserved among L-group pigments.

Although most members in L-group exhibit the chloride effect, some pigments such as mouse green show no chloride effect.¹¹ Mouse green has an absorption maximum at 511 nm, and depletion of chloride or its replacement with nitrate causes no shift of the absorption maximum. Loss of chloride effect in mouse green has been attributed to the presence of a tyrosine residue instead of a histidine at position 181.¹¹ However, it was reported that rodent blind mole rat (*Spalax ehrenbergi*) has an L-group pigment which contains tyrosine at position 181 but shows 12 nm chloride effect.¹² This indicates that replacement of histidine with tyrosine at position 181 is not the sole cause of loss of the chloride effect in mouse green. Recently, we performed a comprehensive mutational analysis of position 181 in crab-eating macaque (*Macaca fascicularis*; mfas) green and found that H181Y mutant of the pigment retained a small but

Received: November 30, 2012

Revised: January 25, 2013

Published: January 25, 2013

significant chloride effect (11 nm).¹³ In the present study, we first explored an L-group pigment other than that of blind mole rat, which has a tyrosine at position 181 and exhibited a chloride-dependent spectral red-shift. We found that the L-group pigment from guinea pig fulfills the criteria. We then searched for amino acid residues which are conserved in L-group pigments of blind mole rat and guinea pig but not in that of mouse green and identified the amino acid residues at positions 289 and 292 responsible for the chloride effect. In addition, we confirmed that replacements at these two residues reciprocally convert the absorption maxima and the chloride effects of guinea pig and mouse pigments. Furthermore, we found that about 80% of the chloride-dependent red-shift disappeared by introducing triple mutations into positions 181, 289, and 292 of mfas green and red. On the other hand, chimerical analysis between mfas green and mouse green showed that residual 20% of the chloride effect could be attributed to the difference in helical arrangements rather than specific amino acids. Based on these results, the molecular mechanism of the chloride effect in L-group cone visual pigments is discussed.

MATERIALS AND METHODS

Preparation of Wild-Type and Mutant Pigments. The cDNAs of mouse green (NCBI accession number; AF011389), guinea pig green (AF132042), and mfas red and green (AF158968 and AF158975) were tagged by the epitope sequence (ETSQVAPA) of the antiovine rhodopsin monoclonal antibody Rho1D4 at the C-terminus and were inserted into the mammalian expression vector, pcDLSR α 296¹⁴ or pcDNA3.1 (Life Technologies). Site-directed mutants were prepared by using the QuikChange kit (Agilent Technologies) according to the manufacturer's instructions. The plasmid DNAs were transfected into HEK293T cells by the calcium phosphate method. After incubation of the transfected cells for 2 days, they were collected by centrifugation and were incubated with 11-*cis*-retinal for more than 3 h at 4 °C to reconstitute the pigments. The pigments were extracted with 0.75% CHAPS and 1 mg/mL phosphatidylcholine containing 50 mM HEPES (pH 6.5), 140 mM NaCl or NaNO₃, and 3 mM MgCl₂ or Mg(NO₃)₂ and were purified with Rho1D4-conjugated agarose. All procedures were performed under dim red light.

Absorption Maxima of Pigments. Absorption spectra were recorded at 0 °C with a Shimadzu UV-2400 spectrophotometer. The pigments were irradiated with light through a glass cutoff filter (VY52, Toshiba) for over 1 min. Difference spectra were calculated from the spectra recorded before and after irradiation in the presence of 2.5 mM hydroxylamine, and the absorption maxima of the pigments in the dark state were estimated based on the difference spectra.

RESULTS

Reciprocal Conversion of Chloride Effect between Mouse Green and Guinea Pig Green. Figure 1 shows the absorption spectra of chloride- and nitrate-bound forms of mouse green and guinea pig green. As previously reported,¹¹ mouse green had absorption maxima at 511 and 510 nm in the presence of chloride and nitrate, respectively, indicating that mouse green shows little chloride effect. On the other hand, guinea pig green had absorption maxima at 524 and 512 nm in the presence of chloride and nitrate, respectively. Thus, guinea

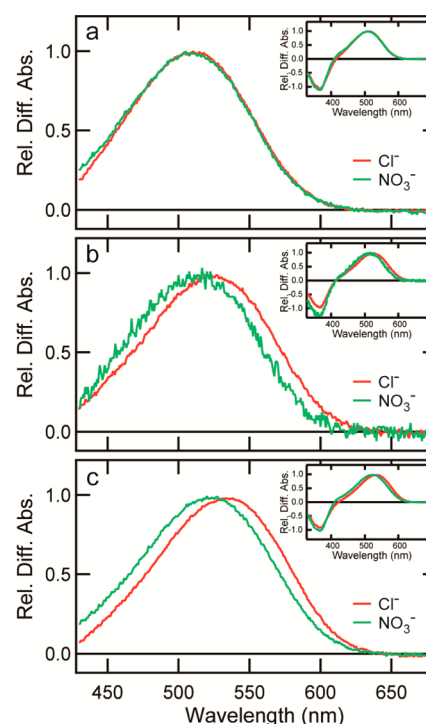


Figure 1. Comparison of the absorption maxima of mouse green and guinea pig green in the presence of chloride or nitrate. Difference absorption spectra were obtained in mouse green (a), guinea pig green (b), and guinea pig green S164A/A269T mutant (c). Red and green spectra were measured under chloride and nitrate saturated conditions, respectively.

pig green shows a significant chloride effect. It has been revealed that amino acid residues situated at three positions, 164, 261 and 269, contribute to the spectral tuning of L-group pigments.^{15,16} Mouse green has amino acid residues Ala, Tyr, and Thr at these positions, whereas guinea pig green has Ser, Tyr, and Ala (Figure S1). Thus, we replaced amino acid residues of guinea pig green at positions 164 and 269 with those of mouse green. This mutant (S164A/A269T) of guinea pig green exhibited absorption maxima at 533 and 522 nm in the presence of chloride and nitrate, respectively (Figure 1c). The chloride effect in this mutant is identical with that in wild-type guinea pig green within our experimental error (Table 1). Hereafter, we refer to this mutant as GP green.

To identify the amino acid residue(s) responsible for the chloride effect, we searched for the residue(s) which are conserved among blind mole rat green, GP green, and mfas green but not in mouse green. Because chloride would be present near the residue at position 181, we compared the residues situated within 8 Å of the residue at position 181 based on the 3D structure of bovine rhodopsin.¹⁷ We found that mouse green has serine residues at positions 289 and 292, whereas the other pigments have alanine residues at these positions (Figure S1). Therefore, we investigated whether or not mutations at these positions of mouse green would result in the chloride-dependent spectral shift.

Figure 2a–d shows absorption spectra of wild-type and mutants of mouse green. The characteristic shift of absorption maximum was observed in single and double mutants. That is, although the absorption maximum of S289A mutant was quite similar to that of wild-type in the chloride-bound form, the mutant showed about 8 nm blue-shift of absorption maximum

Table 1. Absorption Maxima and Chloride Effects of Mouse Green, Guinea Pig Green, and Mfas Red

	$\lambda_{\max}(\text{Cl}^-)$ (nm)	$\lambda_{\max}(\text{NO}_3^-)$ (nm)	$\Delta\lambda_{\max}$ (nm)
mouse green WT	511	509.5	1.5
Y181H/T195S	528	510.5	17.5
Y181H/T276A	527.5	509.5	18
T195S	511	508.5	2.5
T276A	511	509	2
S289A	510	501.5	8.5
S292A	534.5	526.5	8
S289A/S292A	531.5	523.5	8
Y181H/S289A	524.5	503.5	21
Y181H/S292A	552.5	547	5.5
Y181H/S289A/S292A	552	526.5	25.5
guinea pig green WT	523.5	512	11.5
GP green (S164A/A269T)	533	522	11
A289S	533.5	525.5	8
A292S	509.5	498	11.5
A289S/A292S	510.5	508	2.5
mfas red WT	560.5	526.5	34
H181Y	538	517.5	20.5
A289S	561.5	539.5	22
A292S	528	507.5	20.5
H181Y/A289S/A292S	517.5	509	8.5

in the nitrate-bound form. On the other hand, S292A mutant showed a red-shift of absorption maximum in both the chloride- and nitrate-bound forms, but the extent of red-shift in the chloride-bound form was larger than that in the nitrate-bound form, resulting in the chloride-dependent spectral shift (~ 8 nm). The spectral shift of S292A is consistent with the observation in a paper recently published.¹⁸ Absorption maxima of the double mutant (S289A/S292A) were similar to those of single mutant S292A in both the chloride- and nitrate-bound forms but were slightly blue-shifted due to S289A mutation.

Figure 2e–h shows absorption spectra of wild-type and mutants of GP green. We aligned the panels in Figure 2 to show that the pigments in right and left panels have the same amino acid residues at positions 289 and 292. These alignments clearly indicated that the replacements at these two positions have the same effects on the absorption maxima of both mouse green and GP green. That is, the absorption maxima of the chloride- and nitrate-bound forms are quite similar between mouse green and GP green A289S/A292S mutant and between mouse green S289A/S292A mutant and GP green (Table 1). Therefore, the difference in chloride effect between mouse green and GP green is due to the difference in amino acid residues at positions 289 and 292.

Reciprocal Conversion of Chloride Effect between Mouse Green and Mfas Red. The above results clearly

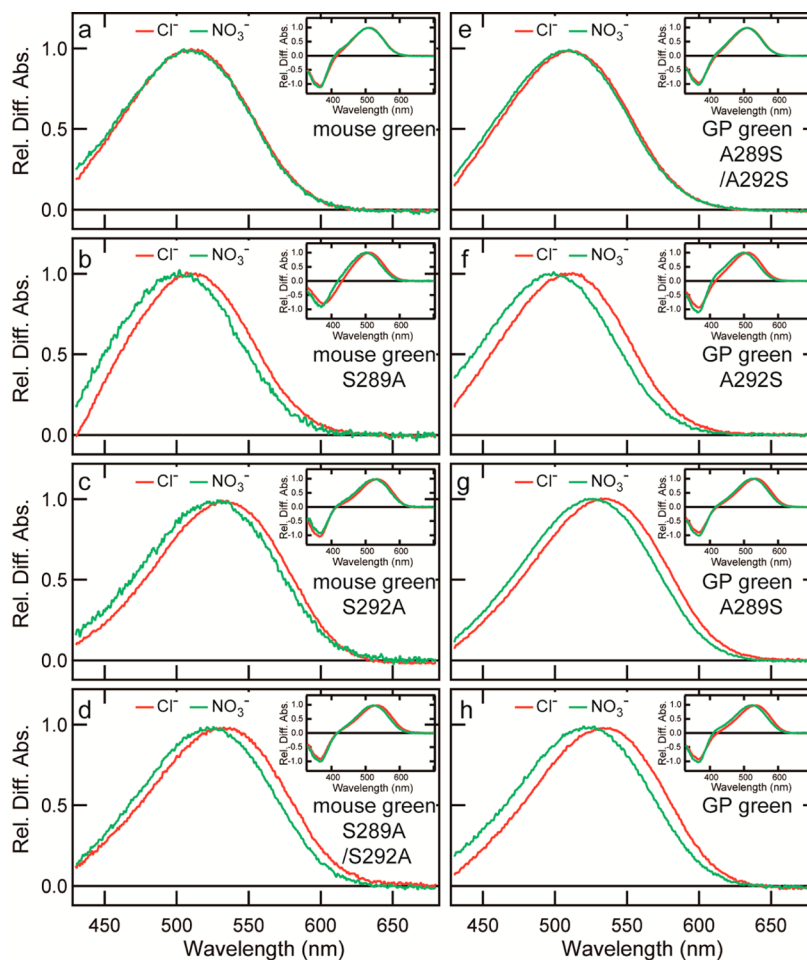


Figure 2. Comparison of the absorption maxima of mouse green and GP green mutants in the presence of chloride or nitrate. Difference absorption spectra were obtained in S289A (b), S292A (c), and S289A/S292A (d) of mouse green (a) and A289S/A292S (e), A292S (f), and A289S (g) of GP green (h). Red and green spectra were measured under chloride and nitrate saturated conditions, respectively.









		λ_{max} (Cl ⁻)(nm)	λ_{max} (NO ₃ ⁻)(nm)	$\Delta\lambda_{\text{max}}$ (nm)			λ_{max} (Cl ⁻)(nm)	λ_{max} (NO ₃ ⁻)(nm)	$\Delta\lambda_{\text{max}}$ (nm)
mouse green WT		511	509.5	1.5	mfas green WT		534	505	29
mouse/mfas (169)		531	504.5	26.5	mfas/mouse (169)		512	510.5	1.5
mouse/mfas (199)		514.5	505	9.5	mfas/mouse (199)		527.5	513	14.5
mouse green Y181H/T195S		528	510.5	17.5	mfas green H181Y		511	497	14

Figure 3. Comparison of the absorption maxima and chloride effects of chimeras between mouse green and mfas green. Absorption maximum was estimated from difference absorption spectrum measured in the presence of chloride or nitrate.

showed that only two residues at positions 289 and 292 are responsible for the differences in the absorption maximum and the chloride effect between mouse green and GP green. We then tried to identify amino acid residues that cause the difference in the absorption maximum and the chloride effect between mouse green and mfas red.

As shown in Figure S1, the residues at positions 289 and 292 as well as position 181 are different between mfas red and mouse green. That is, mfas red has alanine residues at positions 289 and 292, similar to guinea pig green. Thus, we prepared a series of single mutants and the triple mutants of mouse green and mfas red and investigated their chloride effects. We also prepared a series of double mutants of mouse green, each of which has mutations at two out of three sites (Table 1).

We could not obtain the active protein of single mutant Y181H of mouse green by our expression system, which is consistent with the previous report.¹¹ The presence of different amino acid residue(s) near the residue at position 181 may hamper the stability of Y181H mutant in mouse green. We searched for the amino acid residue(s) which are different between mouse green and mfas red within 8 Å from ECL2 (positions 177–190) based on the 3D structure of bovine rhodopsin. We identified two positions, 195 and 276, where mouse green has threonines and mfas red has serine and alanine, respectively. Then we prepared Y181H/T195S and Y181H/T276A mutants of mouse green and obtained their absorption spectra. Both mutants were successfully expressed in cultured cells and exhibited identical absorption maxima at 528 and 510 nm in the chloride- and nitrate-bound forms, respectively. We also confirmed that single mutation at position 195 or 276 caused no change of the absorption spectra of mouse green. The triple mutant (Y181H/S289A/S292A) of mouse green had absorption maxima at 552 and 526 nm in the chloride- and nitrate-bound forms, respectively. Therefore, introduction of triple mutations at these positions caused a large chloride effect (26 nm), although it is still smaller than the chloride effect observed in mfas red (34 nm). The triple mutant (H181Y/A289S/A292A) of mfas red exhibited absorption maxima at 518 and 509 nm in the chloride- and nitrate-bound forms, respectively. Thus, although the chloride effect was greatly reduced by the triple mutations, a small but significant chloride effect still remained. That is, the triple mutations in mfas red were not able to completely reproduce the spectroscopic properties of mouse green.

We further searched for the differences in amino acid residues between mouse green and mfas red. Two more residues were identified at positions 9 and 287 within 8 Å from

position 181, where mouse green has alanine and valine and mfas red has serine and methionine, respectively (Figure S1). We replaced these amino acids in mfas red but found that these residues did not affect the absorption spectra or the chloride effect of the pigment (data not shown). Taken together, these results strongly suggest that only about 80% of the differences of the absorption maximum and the chloride effect between mouse green and mfas red can be reproduced by mutations at positions within 8 Å from the residue at position 181.

To account for the remaining 20% of the chloride effect, we tried another approach; that is, we constructed chimeras between L-group pigments. Because the purification and characterization of the recombinant protein of mfas green were easier than mfas red in our hands, we prepared chimeras between mouse green and mfas green. We divided the sequences of the pigments at position 169 or 199 (at the N- or C-terminus of ECL2) and prepared four kinds of chimeras (Figure 3). The chimera mouse/mfas(169) indicates that the N-terminal side from position 169 of mouse green is fused with the C-terminal side from position 170 of mfas green. We compared the absorption maxima and the chloride effects of mfas green wild-type, mouse green Y181H/T195S mutant, mouse/mfas(169), and mfas/mouse(199). Because there are only two different amino acid residues in ECL2 between mouse green and mfas green, the mouse green Y181H/T185S mutant corresponds to the mouse green having ECL2 of mfas green. Thus, all the four pigments described above share ECL2 of mfas green. We first compared chloride effects of mouse/mfas(169) and mfas green. The extent of the chloride effect of mfas green wild-type (29.5 nm) is larger than that of mouse/mfas(169) (26.5 nm), indicating that the chloride effect is increased when the N-terminal side from position 169 is replaced from mouse green to mfas green. On the other hand, the extent of the chloride effect of mouse green Y181H/T195S mutant (17.5 nm) is larger than that of mfas/mouse(199) (14.5 nm), indicating that the chloride effect is decreased when the N-terminal side from position 169 is replaced from mouse green to mfas green. The correlation between the sequence of the N-terminal side from position 169 and the chloride effect is dependent on the sequence of the C-terminal side from position 200. These results indicated that there is some interaction between the N-terminal side from position 169 and the C-terminal side from position 200, which regulates the extent of the chloride effect. A similar discrepancy was observed also when we compared mouse green wild-type, mfas green H181Y mutant, mfas/mouse(169), and mouse/mfas(199). Therefore, the residual 20% difference in the chloride effect

between mouse green and mfas green/red is due to the interaction between multiple residues within the helical domains rather than specific amino acid residues.

DISCUSSION

In the present study, we identified the amino acid residues that account for the difference in the chloride effect in rodent L-group cone visual pigments and confirmed that the chloride effect in primate L-group cone visual pigments is also mediated by these residues. Mouse green shows no chloride effect, whereas guinea pig green shows significant chloride effect, despite these pigments sharing a tyrosine residue instead of a histidine at position 181. These properties were completely interconvertible with each other when the two residues at position 289 and 292 were replaced. The triple mutations at positions 181, 289, and 292 of mfas red greatly reduced the extent of the chloride effect but did not fully eliminated it like in mouse green. We showed that the residual difference comes from the distinct helical arrangements of the pigments. In the following, we discuss the molecular mechanism and the molecular evolution of the chloride effect in L-group pigments.

Molecular Evolution of Mouse Green. Figure 4 shows the phylogenetic relationship of L-group cone visual pigments

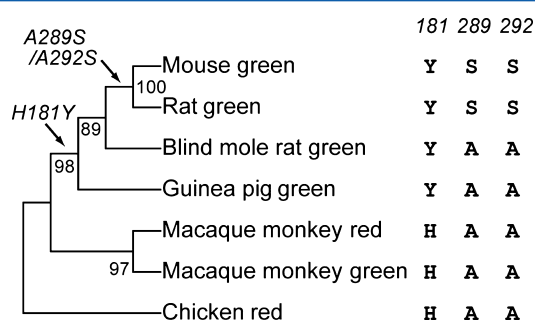


Figure 4. Comparison of three residues based on phylogenetic relationship of L-group pigments. The neighbor-joining tree was constructed using MEGA5.²⁴ NCBI accession numbers of pigment sequences are as follows: rat green, AF054246; blind mole rat green, AF139726; chicken red, X57490.

including rodent ones. Because only a few members from rodents, rabbits, and squirrels contain Tyr181 instead of His181 among L-group pigments,^{11,19,20} we assumed that an ancestral type of L-group pigments had a histidine at position 181. From the phylogenetic tree, it is inferred that the mutations at position 181 and at positions 289 and 292 occurred in a stepwise fashion, which finally resulted in little chloride effect in mouse green. Guinea pig green and blind mole rat green were branched before the mutations at positions 289 and 292, which resulted in a significant chloride effect in these pigments. Although we do not know why mouse green evolved into a pigment with little chloride effect, one possibility is that it may have become blue-shifted to increase the color discrimination ability in conjunction with the UV-sensitive cone visual pigment.²¹

Roles of Amino Acid Residues at Position 181, 289, and 292 on the Chloride-Dependent Red-Shift. The mutations at positions 181, 289, and 292 of mouse green induced chloride-dependent spectral shifts in common and resulted in respective characteristic spectral tuning properties. Figure 5 shows the different effects of the replacements at these residues on the spectral shift of absorption maxima. Y181H

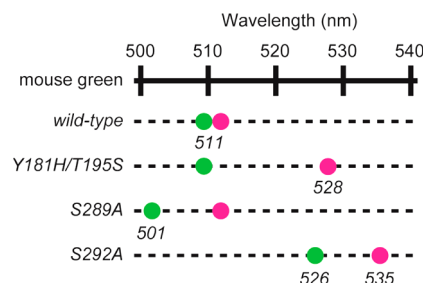


Figure 5. Regulation of chloride effect in mouse green by three residues. Red or green circles represent absorption maxima of mouse green wild-type and mutants in the presence of chloride or nitrate, respectively.

replacement red-shifted the absorption maximum in the chloride-bound form but did not shift the absorbance of the nitrate-bound form. In contrast, S289A replacement blue-shifted the absorption maximum in the nitrate-bound form but did not shift the absorbance of the chloride-bound form. S292A replacement induced a red-shift in both the chloride- and nitrate-bound forms. Previous studies suggested that the nitrate-bound form exhibits absorption maximum similar to that of anion-free form of the pigments.^{6,7} Thus, we compared absorption characteristics of the nitrate-bound form of mouse green and its mutants with those of bovine rhodopsin and its mutants. The nitrate-bound form of mouse green showed no shift of absorption maximum when tyrosine at position 181 was replaced with histidine, which is the same as bovine rhodopsin.²² The spectral red-shift is similar between mouse green and bovine rhodopsin when serine at position 292 was replaced with alanine. However, the extent of red-shift in mouse green (17 nm) is larger than that in bovine rhodopsin (10 nm).¹¹ Additionally, mouse green showed spectral blue-shift when serine at position 289 was replaced with alanine, but bovine rhodopsin showed no shift of absorption maximum by the similar replacement.²³ These results suggested that, although the spatial proximity between the residue at position 181 and the retinal chromophore is similar between mouse green and bovine rhodopsin, the residues at positions 289 and 292 are located closer to the retinal in mouse green than in bovine rhodopsin. In other words, conformation of extracellular region including ECL2 in mouse green is different from that in bovine rhodopsin. In fact, we did not observe any spectral shift when the amino acid residues responsible for the chloride effect in L-group cone visual pigments were introduced to bovine rhodopsin (Figure S2). Analysis of 3D structures of L-group pigments in combination with the quantum mechanical calculations will further our understanding of the molecular mechanism underlying the chloride effect.

ASSOCIATED CONTENT

Supporting Information

The sequence alignment of bovine rhodopsin and L-group cone visual pigments (Figure S1) and the absorption spectrum of bovine rhodopsin mutant (E181H/T289A) (Figure S2). This material is available free of charge via the Internet at <http://pubs.acs.org>.

AUTHOR INFORMATION

Corresponding Author

*Tel +81-75-753-4213, Fax +81-75-753-4210, e-mail shichida@rh.biophys.kyoto-u.ac.jp.

Present Addresses

[†]Graduate School of Frontier Biosciences, Osaka University, Suita, Osaka 565-0871, Japan.

[‡]Department of Biochemistry, University of Toronto, Toronto, ON, Canada M1S5 1A8.

Funding

This work was supported by Grants-in-Aid for Scientific Research (Ministry of Education, Culture, Sports, Science and Technology, Japan) to T.Y. and Y.S. and a Grant for the Global Center of Excellence Program “Formation of a Strategic Base for Biodiversity and Evolutionary Research: from Genome to Ecosystem” (A06).

Notes

The authors declare no competing financial interest.

ACKNOWLEDGMENTS

We thank Dr. S. Koike for providing us with HEK293T cell lines and Prof. R. S. Molday for the generous gift of a Rho1D4-producing hybridoma. We are also grateful to Dr. T. Matsuyama for critical reading of our manuscript and invaluable comments.

ABBREVIATIONS

mfas, *Macaca fascicularis*; ECL2, the second extracellular loop; CHAPS, 3-[(3-cholamidopropyl)dimethylammonio]-propanesulfonate; HEPES, *N*-(2-hydroxyethyl)piperazine-*N'*-2-ethanesulfonic acid; λ_{max} , wavelength at the absorption maximum; WT, wild-type.

REFERENCES

- (1) Shichida, Y., and Imai, H. (1998) Visual pigment: G-protein-coupled receptor for light signals. *Cell. Mol. Life Sci.* 54, 1299–1315.
- (2) Yokoyama, S. (2000) Molecular evolution of vertebrate visual pigments. *Prog. Retinal Eye Res.* 19, 385–419.
- (3) Okano, T., Kojima, D., Fukada, Y., Shichida, Y., and Yoshizawa, T. (1992) Primary structures of chicken cone visual pigments: vertebrate rhodopsins have evolved out of cone visual pigments. *Proc. Natl. Acad. Sci. U. S. A.* 89, 5932–5936.
- (4) Crescitelli, F. (1977) Ionochromic behavior of Grecko visual pigments. *Science* 195, 187–188.
- (5) Fager, L. Y., and Fager, R. S. (1979) Halide control of color of the chicken cone pigment iodopsin. *Exp. Eye Res.* 29, 401–408.
- (6) Shichida, Y., Kato, T., Sasayama, S., Fukada, Y., and Yoshizawa, T. (1990) Effects of chloride on chicken iodopsin and the chromophore transfer reactions from iodopsin to scotopsin and B-photopsin. *Biochemistry* 29, 5843–5848.
- (7) Hirano, T., Imai, H., Kandori, H., and Shichida, Y. (2001) Chloride effect on iodopsin studied by low-temperature visible and infrared spectroscopies. *Biochemistry* 40, 1385–1392.
- (8) Hirano, T., Imai, H., and Shichida, Y. (2003) Effect of anion binding on the thermal reverse reaction of bathiodopsin: anion stabilizes two forms of iodopsin. *Biochemistry* 42, 12700–12707.
- (9) Tachibanaki, S., Imamoto, Y., Imai, H., and Shichida, Y. (1995) Effect of chloride on the thermal reverse reaction of intermediates of iodopsin. *Biochemistry* 34, 13170–13175.
- (10) Wang, Z., Asenjo, A. B., and Oprian, D. D. (1993) Identification of the Cl(–)-binding site in the human red and green color vision pigments. *Biochemistry* 32, 2125–2130.
- (11) Sun, H., Macke, J. P., and Nathans, J. (1997) Mechanisms of spectral tuning in the mouse green cone pigment. *Proc. Natl. Acad. Sci. U. S. A.* 94, 8860–8865.
- (12) Janssen, J. W., David-Gray, Z. K., Bovee-Geurts, P. H., Nevo, E., Foster, R. G., and DeGrip, W. J. (2003) A green cone-like pigment in the ‘blind’ mole-rat *Spalax ehrenbergi*: functional expression and

photochemical characterization. *Photochem. Photobiol. Sci.* 2, 1287–1291.

(13) Morizumi, T., Sato, K., and Shichida, Y. (2012) Spectroscopic Analysis of Chloride Effect on the Active Intermediates of Primate L group Cone Visual Pigment. *Biochemistry* 51, 10017–10023.

(14) Takebe, Y., Seiki, M., Fujisawa, J., Hoy, P., Yokota, K., Arai, K., Yoshida, M., and Arai, N. (1988) SR alpha promoter: an efficient and versatile mammalian cDNA expression system composed of the simian virus 40 early promoter and the R-U5 segment of human T-cell leukemia virus type 1 long terminal repeat. *Mol. Cell. Biol.* 8, 466–472.

(15) Yokoyama, S., and Radlwimmer, F. B. (1998) The “five-sites” rule and the evolution of red and green color vision in mammals. *Mol. Biol. Evol.* 15, 560–567.

(16) Yokoyama, S., and Radlwimmer, F. B. (2001) The molecular genetics and evolution of red and green color vision in vertebrates. *Genetics* 158, 1697–1710.

(17) Okada, T., Fujiyoshi, Y., Silow, M., Navarro, J., Landau, E. M., and Shichida, Y. (2002) Functional role of internal water molecules in rhodopsin revealed by X-ray crystallography. *Proc. Natl. Acad. Sci. U. S. A.* 99, 5982–5987.

(18) Davies, W. I., Wilkie, S. E., Cowing, J. A., Hankins, M. W., and Hunt, D. M. (2012) Anion sensitivity and spectral tuning of middle- and long-wavelength-sensitive (MWS/LWS) visual pigments. *Cell. Mol. Life Sci.* 69, 2455–2464.

(19) Radlwimmer, F. B., and Yokoyama, S. (1998) Genetic analyses of the green visual pigments of rabbit (*Oryctolagus cuniculus*) and rat (*Rattus norvegicus*). *Gene* 218, 103–109.

(20) Yokoyama, S., and Radlwimmer, F. B. (1999) The molecular genetics of red and green color vision in mammals. *Genetics* 153, 919–932.

(21) Yokoyama, S., Radlwimmer, F. B., and Kawamura, S. (1998) Regeneration of ultraviolet pigments of vertebrates. *FEBS Lett.* 423, 155–158.

(22) Yan, E. C., Kazmi, M. A., De, S., Chang, B. S., Seibert, C., Marin, E. P., Mathies, R. A., and Sakmar, T. P. (2002) Function of extracellular loop 2 in rhodopsin: glutamic acid 181 modulates stability and absorption wavelength of metarhodopsin II. *Biochemistry* 41, 3620–3627.

(23) Piechnick, R., Ritter, E., Hildebrand, P. W., Ernst, O. P., Scheerer, P., Hofmann, K. P., and Heck, M. (2012) Effect of channel mutations on the uptake and release of the retinal ligand in opsin. *Proc. Natl. Acad. Sci. U. S. A.* 109, 5247–5252.

(24) Tamura, K., Peterson, D., Peterson, N., Stecher, G., Nei, M., and Kumar, S. (2011) MEGAS: molecular evolutionary genetics analysis using maximum likelihood, evolutionary distance, and maximum parsimony methods. *Mol. Biol. Evol.* 28, 2731–2739.